

Published in final edited form as:

Burns. 2011 May ; 37(3): 377–386. doi:10.1016/j.burns.2010.11.012.

Noninvasive assessment of burn wound severity using optical technology: A review of current and future modalities

Meghann Kaiser^{a,*}, Amr Yafi^b, Marianne Cinat^a, Bernard Choi^b, and Anthony J. Durkin^b

^a Department of Surgery, Division of Trauma, Burns, Critical Care and Acute Care Surgery, University of California, Irvine, Orange, CA 92806, United States

^b Beckman Laser Institute and Medical Clinic, University of California, Irvine, Orange, CA 92806, United States

Abstract

Clinical examination alone is not always sufficient to determine which burn wounds will heal spontaneously and which will require surgical intervention for optimal outcome. We present a review of optical modalities currently in clinical use and under development to assist burn surgeons in assessing burn wound severity, including conventional histology/ light microscopy, laser Doppler imaging, indocyanine green videoangiography, near-infrared spectroscopy and spectral imaging, *in vivo* capillary microscopy, orthogonal polarization spectral imaging, reflectance-mode confocal microscopy, laser speckle imaging, spatial frequency domain imaging, photoacoustic microscopy, and polarization-sensitive optical coherence tomography.

Keywords

Burn; Optical; Laser; Perfusion; Collagen; Partial-thickness; Laser Doppler imaging; Near-infrared; Indocyanine green; Capillary microscopy; Orthogonal polarization spectral; imaging; Reflectance-mode confocal; microscopy; Laser speckle imaging; Spatial frequency domain imaging; Photoacoustic microscopy; Polarization-sensitive optical; coherence tomography

1. Introduction

A half century ago, Dr. Zora Janzekovic and others demonstrated that timely tangential excision and grafting of appropriately deep burns prevented sepsis-related morbidity, diminished the development of hypertrophic burn scars, and radically improved cosmetic and functional outcomes [1–3]. Early excision and grafting of burn wounds thus revolutionized the field of burn surgery and has become a central tenet of the field today [4,5].

The difficulty lies in determining which burn wounds will most benefit from early excision and grafting. Red, painful, non-blistering superficial burns—which do not require excision—are immediately apparent to most clinicians. Likewise, most physicians can identify the pale, leathery, insensate deep burns that must be excised. The gray zone that lies between

© 2010 Elsevier Ltd and ISBI. All rights reserved.

*Corresponding author at: c/o Marianne Cinat, 333 The City Blvd West, Suite 705, Orange, CA 92806, United States. Tel.: +1 714 456 5840; fax: +1 714 456 6048. mkaiser@uci.edu (M. Kaiser).

Conflict of interest

Dr. Anthony Durkin has a financial interest in Modulated Imaging Inc., a company with interests related to spatial field domain imaging (SFDI). Dr. Durkin is a cofounder of the company and owns equity interests in Modulated Imaging.

these extremes consists of “partial-thickness” burns. Some, termed “superficial partial-thickness,” will heal spontaneously in less than two weeks, with minimal or no scarring. Others, categorized as “deep partial-thickness,” will require prompt excision and grafting, without which patients suffer prolonged expensive hospitalizations, painful repetitive dressing changes, and complications such as infections and exacerbated scarring [6–8]. This is the daily challenge of the burn surgeon. Overestimating burn severity could mean unnecessary surgery, underestimation could be just as detrimental.

The stakes are high, and picking the ideal course of treatment is not easy. Most clinicians make their determination on the basis of clinical exam alone. But without additional objective measurements, the judgment alone of even experienced burn surgeons correlates with histology and eventual outcome only about three-quarters of the time [9–13]. As a result, several optical techniques have emerged in recent years to assist in the clinical characterization of burns. Certain modalities provide a means for macroscopic assessment of entire anatomic regions, whereas others enable finely detailed microscopic interrogations of tissue. All share a common theme: visualization of intact dermal vasculature as a measure of viability, whether by visualising the vessel structures themselves or indirectly detecting blood flow. Regardless, each modality offers a unique angle from which to bolster accurate assessment of burn wound depth. Here we review light microscopy, the gold standard of burn wound assessment, as well as both macroscopic and microscopic optical techniques currently in use and under development.

2. *In vitro* light microscopy

Punch biopsy of burn tissue with histologic analysis is still considered the gold standard of burn depth assessment. Thinly sliced tissue specimens are typically stained with hematoxyllin and eosin (H&E stain) and examined under light microscopy. Deep dermal thrombosed blood vessels, sometimes accompanied by denatured collagen, are the hallmarks of deep partial injury on H&E stain [9,13–15]. Use of Masson’s trichome stain under polarized light can assist in differentiating normal collagen—which stains blue—from denatured collagen—red. Verhoeff’s stain of elastin can further demarcate injured from uninjured dermis. Immunostaining may offer an additional edge: anti-vimentin antibody, which labels intact melanocytes and Langerhans’ cells, clearly delineates the zone of necrosis [16]. Antibodies to collagenase, tissue inhibitor of metalloproteinases (TIMP), and collagen IV identify intact, proliferating follicles with the capacity to heal [17,18].

However, even histologic analysis does not absolutely predict eventual clinical outcome. Burn severity can vary greatly over a small area of tissue, rendering punch biopsy vulnerable to sampling errors. The process of obtaining, sectioning, and staining a sample is expensive, time-consuming (on the order of days), and requires the presence of an experienced pathologist. Fixation inevitably leads to artifacts. Perhaps most importantly, biopsy is invasive, guaranteeing discomfort and scarring independent of the burn injury itself. Primarily to address this last shortcoming, a plethora of noninvasive *in vivo* optical techniques has evolved.

3. Macroscopic imaging

3.1. Laser Doppler imaging

Laser Doppler imaging (LDI) typifies the macroscopic imaging modalities and is currently the most widely recognized of the noninvasive, optical burn assessment techniques, with several commercial devices in use internationally. As the name suggests, a laser beam is directed at the tissue, and the frequency of the reflected light, as altered by red blood cells approaching and receding from the detector, indicates the speed and volume of blood flow,

termed “flux,” through an area of interest [19,20]. Based on this information, some commercial devices return a map of different colors calibrated to represent a given area’s specific estimated time to healing, e.g., less than 14 days, 14–21 days, >21 days (Moor Instruments, UK). Thus, similar to light microscopy, LDI cites patent blood vessels as the primary determinant of burn depth, although the focus is on flow rather than the vessels themselves. Not surprisingly then, LDI correlates with burn wound histology and need for surgical excision and grafting about 95% of the time [11–13].

LDI offers obvious advantages over *in vitro* light microscopy. LDI is noninvasive, and in fact can be performed at distances >1 m from the subject with no physical contact whatsoever. The laser energy emitted is harmless. Moreover, a large area can be evaluated, allowing for different management of areas within the same wound [21]. A fairly large body of literature on the subject of LDI speaks to a general comfort level with the device.

LDI is not, however, without its own imperfections. The current commercial device is expensive, large and difficult to position [22]. In our personal experience, between positioning, calibrating, and scanning, evaluation of an area 50 cm × 50 cm may take several minutes, during which the patient must remain motionless to avoid artifact. This can be difficult for anxious or shivering patients and young children in particular, necessitating sedation. The most commonly used commercial device is not promoted for use during the 1st 48 h after injury, secondary to reactive vasoconstriction, and more than 5 days after injury, secondary to the proliferation of granulation tissue [23,24]. Errors can result from vasomotor reactivity and blood pooling in response to second-to-second changes in ambient temperature, patient positioning and emotional states [25] (see Fig. 1). The interpretation of LDI blood flow maps is likewise unclear in the presence of anemia, cellulitis, or peripheral vascular disease. Surface moisture, topical medications, and transparent dressings can also all alter LDI measurements [26]. Where the tissue surface slopes, artifacts may result, making recorded signals difficult to interpret. It is unclear to what extent all this affects the accuracy of LDI, and which wounds are most appropriate for assessment with this modality. Nonetheless, LDI remains an extremely valuable clinical modality for the assessment of burn wounds.

3.2. Indocyanine green (ICG) videoangiography

Indocyanine green is a non-toxic, protein-bound dye that is retained within the vasculature after intravenous injection for several minutes until rapid clearance by the liver. As a diagnostic pharmaceutical, ICG has been in clinical use for decades in the determination of cardiac output. ICG absorbs and fluoresces within the near-infrared spectrum, which has excellent skin penetration, making deeper dermal vasculature visible using this dye [27]. Fluorescence can then be detected, quantified, and digitally translated into color-coded regions of relative perfusion for ease of interpretation, similar to the LDI device (Fig. 2) [28]. Relative to the subject’s normal skin, ICG fluorescence is markedly higher in spontaneously healing wounds, and markedly lower in those that required surgery [29–31]. In a few small human studies, ICG videoangiography findings correlated with histology and/or clinical outcome approaching 100% [30,31].

ICG videoangiography is capable of producing rapid, macroscopic, easily interpreted scans very reminiscent of LDI, on a more compact, less expensive device. In animal studies, it can distinguish deep and deep partial wounds very early, within the first few hours following injury [27]. Its utility has been clearly demonstrated even in the presence of other microvascular pathologies, such as diabetes and heart failure [28]. The primary, obvious drawback of ICG videoangiography is the need for intravascular dye injection. While actually an extremely safe compound, ICG is nonetheless associated with headache, pruritis, urticaria, diaphoresis, and the ever-present risk of life-threatening anaphylactic reaction [32].

Safety has not been well-established in pediatric, pregnant or lactating patients. Additionally, measurements obtained via ICG videoangiography are relative to normal skin controls, and anatomically equivalent regions of normal skin are not always available in burn subjects. The differentiation between normal, decreased, and increased fluorescence can be a very fine line on the order of a few percent making assessment less than clear-cut [27]. Finally, relative to LDI, the body of literature on ICG videoangiography is somewhat small, although a modality with such promise certainly warrants further investigation.

3.3. Near infrared spectroscopy (NIRS)

As mentioned above, near-infrared light can penetrate further into tissue than the visible spectrum, and several biochemically crucial constituents of the dermis absorb wavelengths within the near-infrared spectrum (650–1100 nm). De-oxy hemoglobin has a maximum absorption at 760 nm, whereas absorption of oxy-hemoglobin is greatest at 900 nm. Water, has peak absorption at 980 nm and may have implications for identifying edema. Near-infrared spectroscopy contact probes, termed “point probes” can be geometrically tailored to target specific depths of up to several centimeters in soft tissue [33]. Noncontact near-infrared spectral imaging, which currently represents the majority of NIRS burns research, can generate a map depicting the relative prevalence of these compounds (Fig. 3). Based on the unique reflectance spectra produced by different degrees of injury, models can be derived to significantly predict the presence of superficial partial versus deep partial wounds with an accuracy of 87% in animal models [34].

The ability of NIRS to differentiate between oxygenated and deoxygenated blood confers a distinct theoretical advantage to this modality. LDI detects active blood flow through patent vessels, and assumes that the absence of such blood flow correlates with thrombosed vessels and necrosis. As previously discussed, however, many physiologic states other than thrombosis can temporarily alter blood flow. Deoxy-hemoglobin—present even in thrombosed vessels—may be pivotal in discerning thrombosis from reactive vasoconstriction. Moreover, NIRS spectra reflect not just blood flow, but also the extraction of oxygen from this blood flow. Alterations in cellular metabolism may manifest much sooner after an insult than blood vessel injury and thrombosis, potentially allowing for dramatically earlier injury grading and treatment, on the order of hours rather than days [14,35,36]. Even the degree of inflammation—manifest as edema secondary to capillary leakage—may differ subtly between superficial partial and deep partial wounds [37]. Finally, some NIRS devices have the potential to detect denatured collagen as light scattering [38]. Integrating data on the prevalence of all these molecules—oxy-hemoglobin, de-oxyhemoglobin, water, and denatured collagen—improves the predictive reliability of NIRS [35].

On the other hand, like LDI, scans may take several minutes to complete. Scanning may entail physical probe contact with the wound, causing discomfort for some patients, although noncontact imaging is now commonly used for burn purposes [34,37]. To date, NIRS has reliably differentiated only superficial from full thickness burns in human subjects, not superficial partial from deep partial, which is a much finer line [39]. And, while the variety of device designs, wavelengths, and analysis algorithms possible allow for an enviable degree of customization, there is also a distinct lack of standardization. The full capacity of NIRS in the diagnosis of burn injury is promising but as yet, incompletely elucidated.

4. Microscopic imaging

4.1. Capillary microscopy

Like all the above modalities, transcutaneous *in vivo* capillary videomicroscopy estimates burn wound depth based on the presence of functioning dermal vasculature. The ability of capillary microscopy to accurately assess dermal capillaries has been verified in a number of other disease states affecting skin circulation, including diabetes, chronic venous insufficiency, and psoriasis [40]. In the case of burn injuries, a 200× lens is applied to a small ($\approx 1 \text{ mm}^2$) area of interest and the superficial dermal capillary plexus—filled with red, oxygenated blood cells—easily examined under the visible blue-green spectrum. Intravascular injection of sodium fluorescein dye, and examination under a conventional fluorescence filter with excitation 450–500 nm, may serve to further accentuate the presence or absence of viable vessels [40,41]. The presence of an intact, working plexus implies only superficial or superficial partial injury, whereas a less robust or entirely absent capillary network denotes deep partial or deep injuries (Fig. 4). In one paper, a simple grading system (0–3) of relative capillary destruction without use of fluorescein was developed that correlated with both LDI and clinical outcome in 100% of subjects tested [22].

The capillary microscopy device is relatively inexpensive ($\approx \$10,000$) and portable. It is unaffected by curved skin surfaces and does not require patients to be still for more than seconds at a time. However, it does require direct contact with the burn wound, and can visualize only a very small portion of the wound at once, leaving it vulnerable to sampling error, albeit less so than traditional histology. Interpretation of microscopic findings requires a certain level of expertise, and is to some extent subjective. Most importantly, extensive studies of capillary microscopy in the burns arena are lacking, with only one group having published results to date [22]. It is unclear how soon after injury videomicroscopy is accurate, or how infection and comorbidities might affect measurements. Use in children younger than 13 has not been explored, although such individuals make up a sizable portion of the burn population. Finally capillary microscopy is not normalized to account for expected regional differences in perfusion. An area such as the face with particularly dense dermal vasculature may undergo mild capillary damage and still appear within normal limits. All these issues must be more thoroughly evaluated before capillary microscopy comes to the forefront of burn wound assessment.

4.2. Orthogonal polarization spectral imaging (OPSI)

Orthogonal polarization spectral imaging is a specialized form of *in vivo* transcutaneous videomicroscopy. Polarized light of around 548 nm (well absorbed by hemoglobin) is directed at the tissue, and reflected light is gathered through a second polarization filter perpendicular to the first. Any light permitted through the second filter must encounter multiple scattering surfaces, rendering it no longer at right angles to the filter. Thus superficial structures are eliminated from the image and blood vessels around 3 mm deep—highlighted by the presence of red blood cells absorbing the incident light—are very apparent. With this technology, resolution is sufficient to image the movement of a single red blood cells transversing a capillary in real-time. Circulatory patterns distinct for healing and nonhealing burn wounds can be observed (Fig. 5) [43]. OPSI visualizes both the form and function of dermal capillaries to determine an index of “functional capillary density” (FCD), or the length of perfused vessels in cm per cm^2 of wound examined [44,45]. In one study, setting the threshold for deep partial thickness burns at an FCD of 100 cm/cm^2 detected need for operative intervention with a sensitivity of 93% [45].

Like transcutaneous videomicroscopy, OPSI is relatively inexpensive, portable, unaffected by skin curvature and does not require the subject to remain completely still [45]. FCD is

arguably a much more objective and reproducible measure of the capillary plexus than the relative grading system used for transcutaneous videomicroscopy. Given the unique optics of this technology, the injection of fluorescein—with any small but real associated risks—is not necessary to attain an impressive level of contrast. Thrombosis can be physically distinguished from vasoconstriction [42], allowing different causes of low-flow states to be discerned. Capillaries can be differentiated from larger venules and arterioles, theoretically adding a level of precision to the microscopic determinations of burn wound depth.

However, it is not at all clear that such detail and precision is necessary, and the extra information adds layers of complexity to data analysis. Fields of view are small ($\approx 1 \text{ mm}^2$). Since not every functioning capillary will contain a red blood cell at any given time, thorough examinations take around 15 min to complete, and thereafter must be replayed and meticulously reviewed to accurately assess [45]. FCD improves dramatically between 1 and 4 days post-injury, and the ideal measurement interval has not been established [42,45]. The probe is in direct contact with the burn causing potential discomfort. One can assume that OPSI is affected by comorbidities such as anemia, infection and diabetes [43,44], although it has not been extensively studied in a variety of patient populations. Most importantly, while sensitivity for deep partial and deep burns is high, specificity is low at only around 45% in one study [45]. Furthermore, in this same study, 20% of wounds could not be accurately evaluated due to the presence of edema. Presumably, the extraordinary resolution of OPSI is also its downfall: even slight variations in pressure, whether from interstitial hydrostatic forces or the application of the OPSI probe itself, may cause substantial variation in perceived perfusion. With this sort of inflexibility, OPSI is likely best suited for the research arena at this time.

4.3. Reflectance-mode confocal microscopy (RMCM)

Reflectance-mode confocal microscopy is yet another variation on the transcutaneous videomicroscopy theme. In this version, light from a near-infrared laser is projected at an area of interest, and reflected light received through an aperture of specific diameter. This aperture selects for a specific focal depth by screening out non-focused light and is responsible for a unique feature of RMCM: the ability to view tissue in multiple planes of depth to a maximum of about $350 \mu\text{m}$ [47]. By combining multiple planes, or “optical sections,” a three-dimensional map of the burn wound can be obtained [47,48]. Dermal vessels appear as dark spaces through which bright erythrocytes pass in real time. Other structures helpful in burn wound assessment can also be visualized. Melanin pigment increases reflection and adds contrast, allowing for rapid identification of the epidermal–dermal junction, assuming it is still present post-burn. White blood cells, which proliferate considerably more in deep and deep partial wounds, can be discerned and quantified [46,49]. Also apparent are dermal appendages such as hair follicles, from which epidermal cells regenerate and migrate in the healing wounds [47,48]. Many of these features are significantly different when comparing spontaneously healing and non-healing wounds (Fig. 6) [46,49].

RMCM is a true means of “optical biopsy.” The degree of histologic detail possible may add to the accuracy of depth determination. Serially adjusting the depth of focus allows for a precise determination of the injury’s extent. However, like other forms of transcutaneous videomicroscopy, RMCM requires direct contact with the wound. Miniscule fields ($500 \mu\text{m} \times 500 \mu\text{m}$) are imaged, requiring repetitive measurements at multiple tissue levels to establish a truly representative sampling of the wound—80 fields in one study [46]. This results in a relatively protracted exam of around 10 min, although subjects need not be completely still for the duration. Afterwards, review of the images requires even more time, as well as considerable expertise. Optical sectioning in a plane parallel to the skin surface, as opposed to the perpendicular sectioning of traditional biopsies, makes interpretation more

difficult. RMCM is expensive, at around \$130,000 for a commercially developed device, almost half again the cost of LDI. Most importantly, this modality has not been extensively studied in human burn subjects. No absolute thresholds for differentiating superficial partial thickness burns from deep partial thickness burns are yet established, only relative changes over time in blood flow and white cells. Accuracy, sensitivity and specificity are unknown, undermining its practical applications in decision-making for the average burn surgeon. Like OPSI, RMCM raises some fascinating possibilities but is far from ready for widespread routine clinical use.

4.4. Future modalities

Many other promising optical techniques for the assessment of burn wound depth await human trials, and though clinical data is sparse at this time, it behooves dedicated burn surgeons to familiarize themselves with emerging modalities of such potential. Some represent conceptual improvement on current modalities that measure tissue perfusion. Laser speckle imaging (LSI) creates a speckle image with laser light reflecting off wound bed structures. By capturing two images within milliseconds of one another, speckles appear to “smear” in a manner analogous to increasing exposure time on a conventional camera. The degree of smearing corresponds to the speed and volume of red blood cells. As a result, LSI creates a color-coded map similar to LDI without the prolonged scanning time. LSI assessment of microvasculature has been documented in port-wine stains and other pathologic and physiologic states [50–52]. Our group is currently investigating the use of LSI in human subjects with burns (Fig. 7).

Spatial frequency domain imaging (SFDI) represents the next generation of NIRS. “Spatial frequencies” refer to different patterns of near-infrared light used to illuminate the tissue and specify particular depths of penetration, analogous to the aperture of confocal microscopy. Using these patterns, absorbance of certain relevant wavelengths, such as the peak absorbance of oxy-hemoglobin, deoxy-hemoglobin, and water, can be measured at different depths, creating a three-dimensional map of both the perfusion and metabolic activity within a tissue. Changes in scattering that result from the denaturation of collagen can also be quantified. SFDI can be adjusted to measure areas ranging from 1 cm² to in excess of 100 cm² and, unlike many other NIRS-based devices, does not require any physical contact with the wound. Animal studies with SFDI show clear distinction between superficial and deep wounds [36,53]. A study of SFDI now underway in human burn wounds has produced preliminary findings echoing those of animals (Fig. 8).

Photoacoustic microscopy (PAM) is based on the principal that objects reflecting light energy vibrate as the energy undergoes conversion to heat, emitting sound waves. These sound waves can be picked up by an ultrasonic detector. By projecting a wavelength of light at hemoglobin’s peak absorption, inflamed, hyperemic tissue appears dark (hypoechoic) on PAM, while surrounding tissues reflecting such light waves appear bright (hyperechoic). The result is an image very similar to conventional sound-based ultrasonography, but on a microscopic scale proportional to the much shorter wavelength of light [54]. In an experimental model of burns, PAM was able to distinguish different durations of thermal exposure within minutes of injury [55].

Collagen in its native state is birefringent, or capable of splitting light into two rays polarized perpendicular to one another. When collagen is denatured by thermal injury, it loses this property [56]. Polarization-sensitive optical coherence tomography (PSOCT) quantifies tissue damage according to the degree of polarization in reflected light, detected as phase retardance. The phase retardance of tissues at different tissue levels can be quantified to demarcate injured from uninjured tissues. Animal studies show a statistically strong mathematical correlation between PSOCT measurements and absolute burn depth as

determined by histology [57,58]. This last modality thus differs from the previous modalities discussed in that it is entirely dependent on the structure of collagen, not the microvasculature, for burn depth assessment.

5. Conclusion

The ability to predict which burn wounds will heal spontaneously and which will require surgical intervention is a critical component of clinical treatment algorithms. Gross clinical exam alone is accurate only about three-quarters of the time. Current optical techniques to complement clinical exam operate on the premise that functioning blood vessels are retained in viable tissue. Both macroscopic and microscopic modalities are available, offering different advantages and disadvantages. While many questions remain to be answered, experience to date indicates that the field of optics will contribute an invaluable degree of accuracy and insight to the field of burn assessment.

Acknowledgments

Drs. Durkin and Yafi acknowledge salary support provided by the NIH NCRR Laser and Medical Microbeam Program, (LAMMP: 5P-41RR01192); the Military Photomedicine Program, (AFOSR Grant # FA9550-08-1-0384), the Beckman Foundation and the Hazem Chehabi BLI Research Fellowship.

References

1. Janzekovic Z. A new concept in the early excision and immediate grafting of burns. *J Trauma*. 1970; 10(12):1103–8. [PubMed: 4921723]
2. Cramer LM, McCormack RM, Carroll DB. Progressive partial excision and early grafting in lethal burns. *Plast Reconstr Surg Transplant Bull*. 1962; 30:595–9. [PubMed: 14023665]
3. Meeker IA, Snyder WH. Dermatome debridement and early grafting of extensive third degree burns in children. *Surg Gynecol Obstet*. 1956; 103(5):527–34.
4. Saffle JR. Practice guidelines for burn care. *J Burn Care Rehabil*. 2001; 22(Suppl 1)
5. Orgill DP. Excision and skin grafting of thermal burns. *N Engl J Med*. 2009; 360(9):893–901. [PubMed: 19246361]
6. Engrav LH, Heimbach DM, Reus JL, Harnar TJ, Marvin JA. Early excision and grafting vs. nonoperative treatment of burns of indeterminate depth: a randomized prospective study. *J Trauma*. 1983; 23(11):1001–4. [PubMed: 6355500]
7. Jackson DM. In search of an acceptable burn classification. *Br J Plast Surg*. 1970; 23(3):219–26. [PubMed: 5469593]
8. Thomsen M, Alsbjorn BF. Development of the treatment of partial skin thickness burns since the second world war: an overview. *Burns*. 1992; 18(Suppl 2):S11–3. [PubMed: 1418516]
9. Gursu KG. An experimental study for diagnosis of burn depth. *Burns*. 1977; 4(2):97–103.
10. Heimbach D, Engrav L, Grube B, Marvin J. Burn depth: a review. *World J Surg*. 1992; 16(1):10–5. [PubMed: 1290249]
11. Niazi ZB, Essex TJ, Papini R, Scott D, McLean NR, Black MJ. New laser Doppler scanner, a valuable adjunct in burn depth assessment. *Burns*. 1993; 19(6):485–9. [PubMed: 8292231]
12. Jeng JC, Bridgeman A, Shivnan L, Thronton PM, Alam H, Clarke TJ, et al. Laser Doppler imaging determines need for excision and grafting in advance of clinical judgment: a prospective blinded trial. *Burns*. 2003; 29(7):665–70. [PubMed: 14556723]
13. Pape SA, Skouras CA, Byrne PO. An audit of the use of laser Doppler imaging (LDI) in the assessment of burns of indeterminate depth. *Burns*. 2001; 27(3):233–9. [PubMed: 11311516]
14. Jackson DM. Second thought on the burn wound. *J Trauma*. 1969; 9(10):839–62. [PubMed: 4898658]
15. Chen B, Thomsen SL, Thomas RJ, Oliver J, Welch AJ. Histological and modeling study of skin thermal injury to 2.0 μm laser irradiation. *Laser Surg Med*. 2008; 40(5):358–70.

16. Nanney LB, Wenczak BA, Lynch JB. Progressive burn injury documented with vimentin immunostaining. *J Burn Care Rehabil.* 1996; 17(3):191–8. [PubMed: 8736363]
17. Ho-Asjoe M, Chronnell CM, Frame JD, Leigh IM, Carver N. Immunohistochemical analysis of burn depth. *J Burn Care Rehabil.* 1999; 20(3):207–11. [PubMed: 10342472]
18. Stricklin GP, Nanney LB. Immunolocalization of collagenase and TIMP in healing human burn wounds. *J Invest Dermatol.* 1994; 103(4):488–92. [PubMed: 7930672]
19. Stern MD. In vivo evaluation of microcirculation by coherent light scattering. *Nature.* 1975; 254(5495):56–8. [PubMed: 1113878]
20. Jaskille AD, Ramella-Roman JC, Shupp JW, Jordan MH, Jeng JC. Critical review of burn depth assessment techniques: part II. Review of laser Doppler technology. *J Burn Care Res.* 2010; 31(1): 151–7. [PubMed: 20061851]
21. Sainsbury DC. Critical evaluation of the clinimetrics of laser Doppler imaging in burn assessment. *J Wound Care.* 2008; 17(5):193–4. 196–8, 200. [PubMed: 18546992]
22. McGill DJ, Sorensen K, MacKay IR, Taggart I, Watson SB. Assessment of burn depth: a prospective, blinded comparison of laser Doppler imaging and videomicroscopy. *Burns.* 2007; 33(7):833–42. [PubMed: 17614206]
23. Moor Instruments, Laser Doppler blood flow assessment. MoorLDI2-BI FAQs. August 21st. 2010 <http://www.moor.co.uk/products/burnassessment/moorldi2/FAQs>
24. Hoeksema H, Van de Sijpe K, Tondu T, Hamdi M, Van Landuyt K, Blondeel P, et al. Accuracy of early burn depth assessment by laser Doppler imaging on different days post burn. *Burns.* 2009; 35(1):36–45. [PubMed: 18952377]
25. Waxman K, Lefcourt N, Achauer B. Heated laser Doppler flow measurements to determine depth of burn injury. *Am J Surg.* 1989; 157(6):541–3. [PubMed: 2658639]
26. Holland AJ, Ward D, Farrell B. The influence of burn wound dressings on laser Doppler imaging assessment of a standardized cutaneous injury model. *J Burn Care Res.* 2007; 28(6):871–8. [PubMed: 17925655]
27. Jerath MR, Schomacker KT, Sheridan RL, Nishioka NS. Burn wound assessment in porcine skin using indocyanine green fluorescence. *J Trauma.* 1999; 46(6):1085–8. [PubMed: 10372631]
28. Kamolz LP, Andel H, Haslik W, Donner A, Winter W, Meissl G, et al. Indocyanine green video angiographies help to identify burns requiring operation. *Burns.* 2003; 29(8):785–91. [PubMed: 14636752]
29. Braue EH, Graham JS, Doxzon BF, Hanssen KA, Lumpkin HL, Stevenson RS, et al. Noninvasive methods for determine lesion depth from vesicant exposure. *J Burn Care Res.* 2007; 28(2):275–85. [PubMed: 17351445]
30. Sheridan RL, Schomaker KT, Lucchina LC, Hurley J, Yin LM, Tompkins RG, et al. Burn depth estimation by use of indocyanine green fluorescence: initial human trial. *J Burn Care Rehabil.* 1995; 16(6):602–4. [PubMed: 8582937]
31. Still JM, Law EJ, Klavuhn KG, Island TC, Holtz JZ. Diagnosis of burn depth using laser-induced indocyanine green fluorescence: a preliminary clinical trial. *Burns.* 2001; 27(4):364–71. [PubMed: 11348745]
32. Benya R, Quintana J, Brundage B. Adverse reactions to indocyanine green: a case report and a review of the literature. *Cathet Cardiovasc Diagn.* 1989; 17(4):231–3. [PubMed: 2670244]
33. Cerussi AE, Jakubowski D, Shah N, Bevilacqua F, Lanning R, Berger AJ, et al. Spectroscopy enhances the information content of optical mammography. *J Biomed Opt.* 2002; 7(1):60–71. [PubMed: 11818013]
34. Sowa MG, Leonardi L, Payette JR, Cross KM, Gomez M, Fish JS. Classification of burn injuries using near-infrared spectroscopy. *J Biomed Opt.* 2006; 11(5):054002. [PubMed: 17092151]
35. Sowa MG, Leonardi L, Payette JR, Fish JS, Mantsch HH. Near infrared spectroscopic assessment of hemodynamic changes in the early post-burn period. *Burns.* 2001; 27(3):241–9. [PubMed: 11311517]
36. Yafi A, Vetter TS, Pharaon MR, Scholz T, Patel S, Saager RB, et al. Postoperative quantitative assessment of reconstructive tissue status in cutaneous flap model using spatial frequency domain imaging. *J Plast Reconstr Surg.* 2011 (in press).

37. Cross KM, Leonardi L, Gomez M, Freisen JR, Levasseur MA, Schattka BJ, et al. Noninvasive measurement of edema in partial thickness burn wounds. *J Burn Care Res.* 2009; 30(5):807–17. [PubMed: 19692905]
38. Weingarten MS, Papazoglou ES, Zubkov L, Zhu L, Neidrauer M, Savir G, et al. Correlation of near infrared absorption and diffuse reflectance spectroscopy scattering with tissue neovascularization and collagen concentration in a diabetic rat wound healing model. *Wound Repair Regen.* 2008; 16(2):234–42. [PubMed: 18318809]
39. Ross KM, Leonardi L, Payette JR, Gomez M, Mevasseur MA, Schattka BJ, et al. Clinical utilization of near-infrared spectroscopy devices for burn depth assessment. *Wound Repair Regen.* 2007; 15(3):332–40. [PubMed: 17537120]
40. Hern S, Mortimeter PS. Visualization of dermal blood vessels—capillaroscopy. *Clin Exp Dermatol.* 1999; 24(6):473–8. [PubMed: 10606953]
41. Peled IJ, Har-Shai Y, Ullman Y. Fluorescein and burn depth. *Burns.* 1993; 19(1):90. [PubMed: 8435127]
42. Milner SM, Bhat S, Gulati S, Gherardini G, Smith CE, Bick RJ. Observations on the microcirculation of the human burn wound using orthogonal polarization spectral imaging. *Burns.* 2005; 31(3):316–9. [PubMed: 15774287]
43. Groner W, Winkelman JW, Harris AG, Ince C, Bouma GJ, Messmr K, et al. Orthogonal polarization spectral imaging: a new method for study of the microcirculation. *Nat Med.* 1999; 5(10):1209–12. [PubMed: 10502828]
44. Winkelman JW. Noninvasive blood cell measurements by imaging of the microcirculation. *Am J Clin Pathol.* 2000; 113(4):479–83. [PubMed: 10761448]
45. Goertz O, Ring A, Kohlinger A, Daigeler A, Andree C, Steinau HU, et al. Orthogonal polarization spectral imaging: a tool for assessing burn depths? *Ann Plast Surg.* 2010; 64(2):217–21. [PubMed: 20098109]
46. Altintas MA, Altintas AA, Knobloch K, Guggenheim M, Zweifel CJ, Vogt PM. Differentiation of superficial partial vs. deep partial thickness burn injuries in vivo by confocal-laser scanning microscopy. *Burns.* 2009; 35(1):80–6. [PubMed: 18691820]
47. Calzavara-Pinton P, Longo C, Venturini M, Sala R, Pellacani G. Reflectance confocal microscopy for in vivo skin imaging. *Photochem Photobiol.* 2008; 84(6):1421–30. [PubMed: 19067964]
48. Rajadhyaksha M, Gonzalez S, Zavislan JM, Anderson RR, Webb RH. In vivo confocal scanning laser microscopy of human skin II: advances in instrumentation and comparison with histology. *J Invest Dermatol.* 1999; 113(3):293–303. [PubMed: 10469324]
49. Altintas AA, Guggenheim M, Altintas MA, Amini P, Stasch T, Spilker G. To heal or not to heal: predictive value of in vivo reflectance-mode confocal microscopy. *J Burn Care Res.* 2009; 30(6):1007–12. [PubMed: 19826264]
50. Huang YC, Tran N, Shumaker PR, Kelly K, Ross EV, Nelson JS, et al. Blood flow dynamics after laser therapy of port-wine stain birthmarks. *Lasers Surg Med.* 2009; 41(8):563–71. [PubMed: 19731304]
51. Cheng H, Luo Q, Liu Q, Lu Q, Gong H, Zeng S. Laser speckle imaging of blood flow in microcirculation. *Phys Med Biol.* 2004; 49(7):1347–57. [PubMed: 15128210]
52. Boas DA, Dunn AK. Laser speckle contrast imaging in biomedical optics. *J Biomed Opt.* 2010; 15(1):011109. [PubMed: 20210435]
53. Pharaon MR, Scholz T, Bogdanoff S, Cuccia D, Durkin AJ, Hoyt DB, et al. Early detection of complex vascular occlusion in a pedicle flap model using quantitative spectral imaging. *Plast Reconstr Surg.* 2010; 126(6):1924–35. [PubMed: 21124132]
54. Zhang HF, Maslov K, Stoica G, Wang LV. Imaging acute thermal burns by photoacoustic microscopy. *J Biomed Opt.* 2006; 11(5):054033. [PubMed: 17092182]
55. Zhang HF, Maslov K, Stoica G, Wang LV. Functional photoacoustic microscopy for high-resolution and noninvasive in vivo imaging. *Nat Biotechnol.* 2006; 24(7):848–51. [PubMed: 16823374]
56. Thomsen S, Pearce JA, Cheong WF. Changes in birefringence as markers of thermal damage in tissues. *IEEE Trans Biomed Eng.* 1989; 36(12):1174–9. [PubMed: 2606492]

57. Srinivas SM, de Boer JF, Park H, Keikhanzadeh K, Huang HE, Zhang J, et al. Determination of burn depth by polarization-sensitive optical coherence tomography. *J Biomed Opt.* 2004; 9(1): 207–12. [PubMed: 14715075]
58. Park BH, Saxer C, Srinivas SM, Nelson JS, de Boer JF. In vivo burn depth determination by high-speed fiber-based polarization sensitive optical coherence tomography. *J Biomed Opt.* 2001; 6(4): 474–9. [PubMed: 11728208]

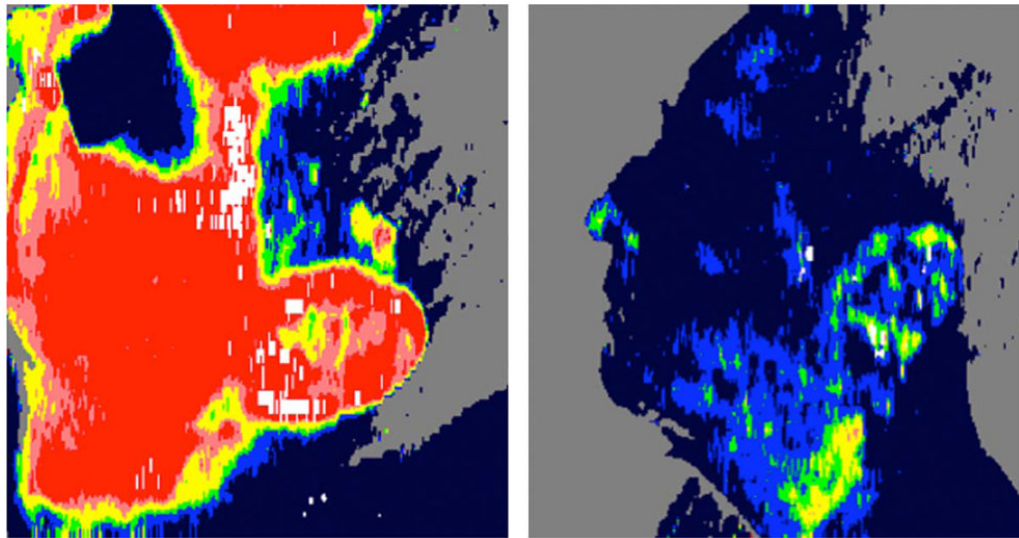


Fig. 1.

On the left, LDI-generated blood flow map of a superficial partial thickness burn on a patient's face. High blood flow is manifest as a predominantly bright red region. On the right, the same area on the same patient minutes later, showing significantly diminished perfusion, as suggested by the now dark blue facial area. Shortly after the second scan, the patient experienced a near-syncopal episode. (For interpretation of the references to color in this figure legend, the reader is referred to the web version of the article.)

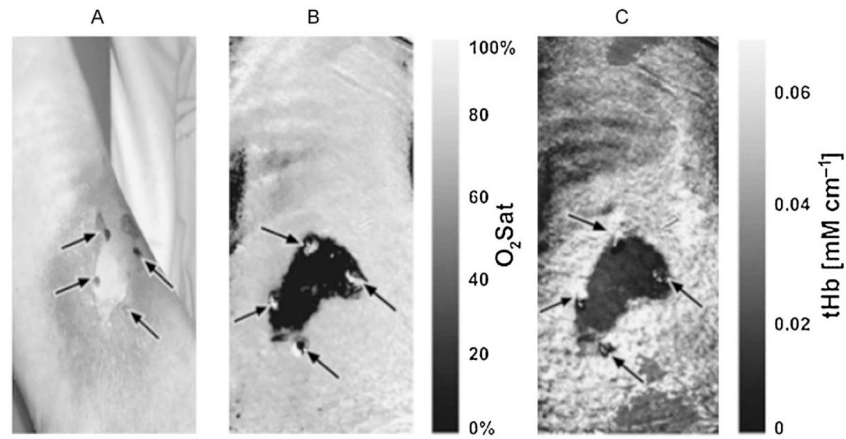


Fig. 2. Near-infrared spectral imaging. (A) Digital photograph of burn wound to the leg with central area of full thickness. (B) Map of tissue oxygen saturation with darker areas representing less oxygenation, corresponding to full thickness injury. (C) Map of total hemoglobin concentration with darker areas representing less hemoglobin. (Reprinted from Ref. [40]. Copyright 2007 by John Wiley and Sons. Reprinted with permission.)

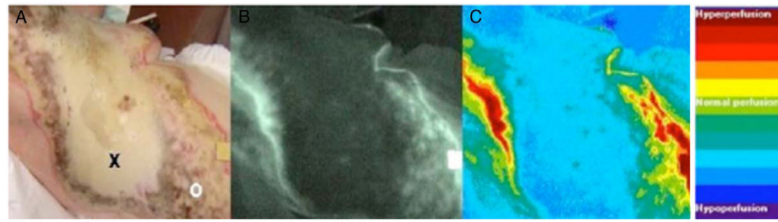


Fig. 3.

Indocyanine green video angiography. (A) Digital photograph of a burn to the chest with central area of full thickness (x) and peripheral areas of partial thickness (o). (B) Raw angiography image with brighter areas corresponding to regions of increased perfusion. (C) Computer generated image quantifying fluorescence with areas of greater perfusion represented by red and less perfusion by blue. (Reprinted from Ref. [29]. Copyright 2003 by Elsevier. Reprinted with permission.) (For interpretation of the references to color in this figure legend, the reader is referred to the web version of the article.)

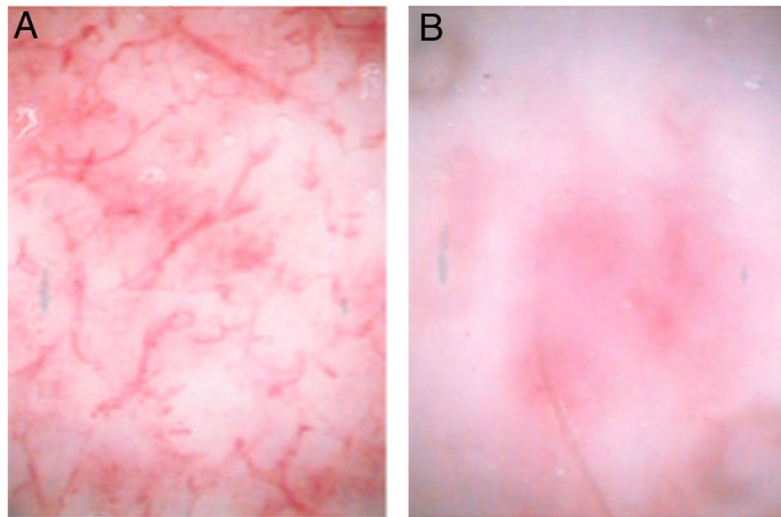


Fig. 4. *In vivo* capillary microscopy. (A) Superficial burn with preserved dermal capillary plexus visible. (B) Deep partial thickness burn with absence of the capillary plexus apparent. (Reprinted from Ref. [22]. Copyright 2007 by Elsevier. Reprinted with permission.)

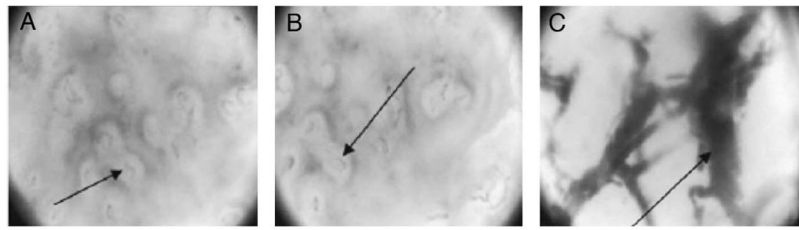


Fig. 5. Orthogonal polarization spectral imaging. (A) Normal skin, in which the dermal capillary plexus is apparent as faint gray loops. (B) Superficial burn, appearing very similar to normal skin. (C) Deep burn, in which the destruction of the overlying capillary plexus allows for visualization of the larger thrombosed dermal vessels beneath. (Reprinted from Ref. [43]. Copyright 2005 by Elsevier. Reprinted with permission.)

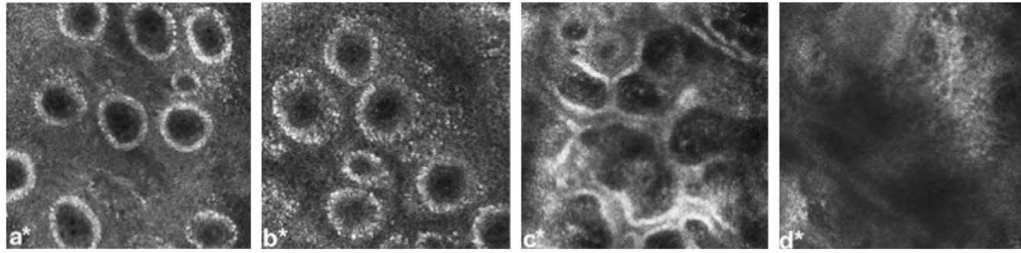


Fig. 6.

Reflectance confocal microscopy of a human subject at 24 h post-injury showing (a) normal skin, with dermal capillaries manifested as black punctate areas within dermal papillae (white rings), (b) superficial burn, with apparent enlargement of the dermal capillaries secondary to edema, (c) superficial partial-thickness burn, showing incomplete destruction of the dermal papillae, and (d) deep partial-thickness burn, showing complete destruction of the papillae. (Reprinted from Ref. [47]. Copyright 2009 by Elsevier. Reprinted with permission.)

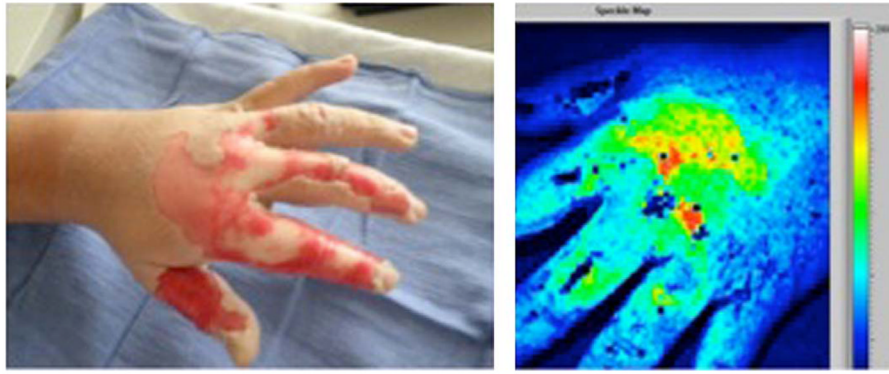


Fig. 7. On the left, a digital photograph of a hot oil burn to the hand with areas of deep (white) and partial (pink) thickness. On the right, the laser speckle image (LSI) of the same burn. Areas of high perfusion are represented by brighter colors (red, yellow, green, in order of decreasing perfusion) and lower perfusion is represented by blue. Deep thickness regions on the proximal second, third, and fourth digits correspond to light blue areas on the speckle image, whereas the dorsum of the hand overlying the metacarpals is partial thickness on clinical exam green/yellow/red on the speckle image. Uninjured, non-inflamed skin is blue. (Patient permission was obtained to publish photograph.) (For interpretation of the references to color in this figure legend, the reader is referred to the web version of the article.)

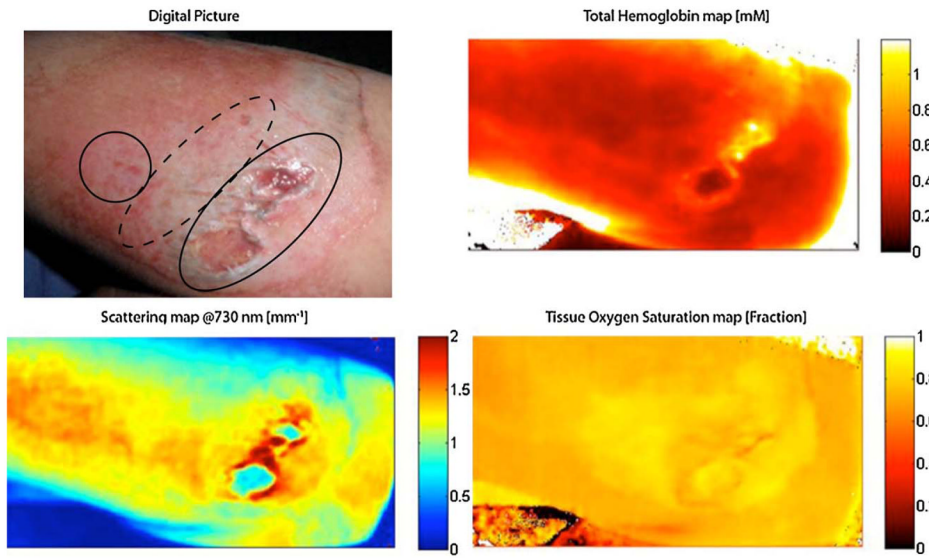


Fig. 8. In the upper left corner, a digital photograph of mechanical burn (road rash) to the forearm with areas of full (oval), deep partial (dashed oval), and superficial partial (circle) thickness injury. Regional maps of hemoglobin, oxygen saturation, and light scattering can differentiate between different depths within the wound as shown (patient permission was obtained to publish photograph).